Applied Catalysis B: Environmental 185 (2016) 253–264

Contents lists available at ScienceDirect

Applied Catalysis B: Environmental

journal homepage: www.elsevier.com/locate/apcatb

Transesterification of vegetable oils by $AlPO_xN_y$ heterogeneous catalysts

Franck Tessier[a,*], Erwan Ray[a], François Cheviré[a], Laurent Lemaître[b], Fabien Bonnier[b], Delphine Bazer-Bachi[b], Vincent Lecocq[b]

[a] Institut des Sciences Chimiques de Rennes (UMR CNRS 6226), équipe Verres et Céramiques, Université de Rennes 1, F-35042 Rennes cedex, France
[b] IFP Energies nouvelles, Rond-point de l'échangeur de Solaize, BP 3, F-69360 Solaize, France

ARTICLE INFO

Article history:
Received 25 August 2015
Received in revised form 1 December 2015
Accepted 11 December 2015
Available online 15 December 2015

Keywords:
Transesterification
Nitridation
Aluminophosphates
Heterogeneous catalysis
Vegetable oils

ABSTRACT

$AlPO_xN_y$ are the most studied materials among nitrided phosphates in heterogeneous catalysis. Such catalysts were tested in this work for the transesterification reaction of canola oil. High specific surface areas $AlPO_4$ precursors have been prepared using hydrogel or citrate routes. Nitrided powders obtained after thermal reaction under ammonia flow keep high surface areas and nitrogen contents can be modulated depending on the experimental conditions. Both precursor and oxynitrides have been characterized by BET, oxygen and nitrogen analyses, infrared and NMR spectroscopies. The influence of the metal, the alcohol and the nitrogen content on the catalytic performances was also studied. $AlPO_4$ and corresponding nitrided phases (with N wt.% <10) produce higher catalytic activities for the transesterification of vegetable oils compared to that of the reference catalyst $ZnAl_2O_4$.

1. Introduction

Metallic phosphates of the $M^{III}PO_4$ type with M = B, Al, Fe, Ga, Mn form an interesting class of materials [1,2]. Both cations—phosphorus and the metal—are in tetrahedral sites and tetrahedrons are linked to build 3D-networks analogous to those existing in various cristallized polymorphs of silica. Bondings in these MPO_4 phosphates are mainly covalent, with a stronger covalent behavior of phosphate ions compared to that of silicate ones [2]. This family of phosphates has excellent properties, for example in catalysis, as bifunctionnal acid and basic catalysts. They present a significant reactivity for several reactions such as alcohol dehydration, alcenes isomerisation, cracking of aromatic molecules as well as the Knoevenagel condensation [3–9].

The introduction of nitrogen N^{3-} within an oxide catalyst modifies the acid–base properties of the surface and allows to perform catalytic reactions leading to the synthesis of pure chemical substances (aldehydes or sulfones) [10–20]. Steins claimed that the nitrogen/oxygen substitution within a high specific surface area oxide should involve an increase of the Lewis basicity in relation to the lower electronegativity of nitrogen [21]. By tuning the nitrogen content of these materials, the acid–base character can be adjusted to give rise to a large panel of catalytic applications.

"AlPON"-type materials, developed in the early 90's are representative of the most studied nitridophosphates for catalysis [22]. $AlPO_4$ precursors are often prepared using the hydrogel route to form X-rays amorphous and high specific surface areas powders (350–400 $m^2\,g^{-1}$). SEM analysis shows an homogeneous texture with aggregates made of particles with size around tens of nanometers. The oxide precursor is then modified by the progressive nitrogen insertion. "AlPON" results from the reaction of $AlPO_4$ under flowing ammonia between 650 °C and 800 °C and remains X-ray amorphous. A large domain of $AlPO_xN_y$ compositions ($1.5 < x < 4$; $0 < y < 1.65$) exists according to the chosen temperature and nitridation step. Using ammonia temperature programmed desorption (TPD), Conanec has shown a decrease in the acidity of "AlPON" samples with increasing nitrogen content [19,22]. Moreover, under specific experimental conditions, CO_2 TPD enabled to evidence a stronger basic behavior for "AlPON", as observed in the Knoevenagel reaction test [19]. This reaction between a methylenic compound and an aldehyde or a ketone is largely studied as a standard basicity test [23,24]. AlPONs have shown during the condensation reaction of malonitrile or ethylcyanoacetate and benzaldehyde a higher activity compared to that of MgO, a well-known basic catalyst reference. AlPONs present both basic sites originating from amino groups at the surface (—NH—, $—NH_2$) and also acid sites linked to the metal.

* Corresponding author. Fax: +33 223235611.
E-mail address: franck.tessier@univ-rennes1.fr (F. Tessier).

http://dx.doi.org/10.1016/j.apcatb.2015.12.024
0926-3373/

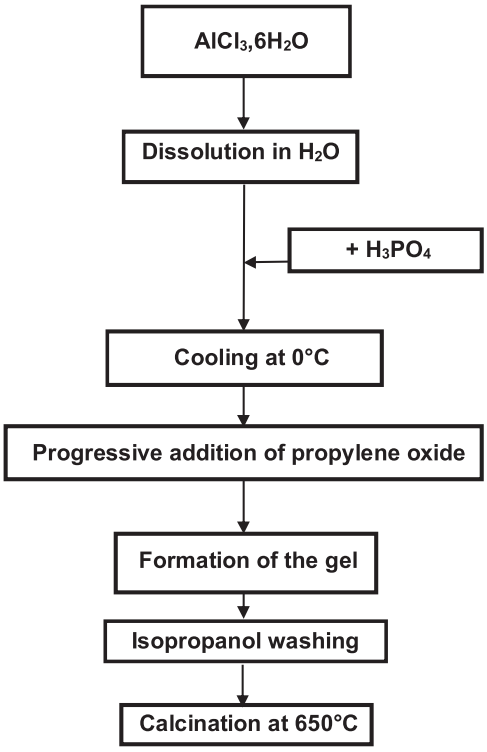

Fig. 1. Synthesis of $AlPO_4$.

Considering the interest of this aluminophosphate family, we have studied the behavior of such heterogeneous catalysts—both $AlPO_4$ and "AlPON"—in the transesterification reaction of vegetable oils. The final products are fatty acid esters (FAME) entering the composition of biodiesel and glycerine, a by-product (generally 10–15 wt.%) that can be further recycled and valued in industry if highly pure. In this work are presented the catalytic performances along with the characterizations of the powders including NMR and infrared spectroscopy.

2. Experimental

2.1. Precursors syntheses

2.1.1. Hydrogel route

This synthesis method was described by Kearby [25] and used in our laboratory by Conanec and Peltier to prepare $AlPO_4$ and $GaPO_4$ [22,26]. Considering the case of $AlPO_4$ (Fig. 1): phosphoric acid H_3PO_4 (1 M) is added in a stoichiometric quantity to an aluminum chloride $AlCl_3$, $6H_2O$ solution. The mixture is then cooled in an ice bath and propylene oxide is poured dropwise in a large excess (3–30 times) under vigorous stirring. The very acidic pH of the solution (pH < 1) increases progressively. Starting from pH ~ 2.5 a thick and translucent gel forms after few hours rest at ambient conditions. The gel is then washed with isopropanol in order to dissolve chlorinated alcohols resulting from the reaction. After several washing steps, the remaining product is dried in an oven during 15 h at 120 °C. After grinding and calcination between 550 and 650 °C the ensuing powder is X-rays amorphous.

2.1.2. Amorphous citrate route

The citrate route is also a method of interest to prepare high specific surface area phosphate precursors [27]. Aqueous solutions of aluminum chloride and ammonium dihydrogen phosphate corresponding to an Al/P ratio = 1 were mixed under stirring. Then, citric acid ($C_6H_8O_7$, Merck, >99%) dissolved in a minimum amount of water was added to each solution, the addition being followed by a 30 min stirring step at 120 °C. Since the complexation of cations by citric acid is improved at pH ≥ 7, the acidic solutions were neutralized using an ammonia solution (25%, Merck) [28]. The solutions were then mixed together and stirred at 150 °C for 20 min to promote chelate formation. The liquid was progressively heated up to 250 °C to eliminate solvents and start the organics combustion, leading after 5 h to an expanded black solid residue. The solid was finally ground and calcined at 550 °C in air in an alumina crucible for elimination of residual carbon. A heating step at 1000 °C during few hours enables to confirm the presence of crystalline $AlPO_4$ with the ratio Al/P = 1.

2.1.3. Thermal ammonolysis

Nitridation reactions were carried out in alumina boats placed inside an electric tubular furnace through which ammonia gas flowed with a flow rate of 20 L h^{-1}. The temperature was raised to 800 °C range at a heating rate of 10 °C min^{-1}. After 15–50 h reaction time, the furnace was switched off and the nitrided powders were allowed to cool to room temperature under nitrogen atmosphere [29].

2.1.4. X-ray diffraction

XRD powder patterns were recorded using a Philips PW3710 diffractometer operating with Cu Kα radiation (λ = 1.5418 Å). X'PERT softwares—Data Collector and Graphics, and Identify—were used, respectively, for pattern recording, analysis and phase matching.

2.1.5. Elemental analysis

Nitrogen and oxygen contents were determined with a LECO® TC-600 analyzer using the inert gas fusion method. Nitrogen was measured as N_2 by thermal conductivity and oxygen as CO_2 by infrared detection. The apparatus was calibrated using Leco® standard oxides, Si_2N_2O and ε-TaN as a nitrogen standard [30]. Nitrogen contents from 6 to 15 wt.% were measured depending on the nitridation temperature. Corresponding chemical formulas were calculated as $AlPO_xN_y$.

Energy-dispersive X-ray analysis (EDX) has been used for identifying the elemental Al:P contents of the products. The EDX analysis system works as an integrated feature of a scanning electron microscope (JEOL JSM 6400).

2.1.6. Specific surface area

A flowsorb II 2300 Micromeritics apparatus was used to determine the specific surface area of the powders by the single point method. Before measurement, the samples were outgassed under He/N_2 flow between 100 and 200 °C for 30 min. Analyses performed with the ASAP 2010 (Micromeritics) give access to the porosimetry, adsorption isotherm and also to the specific surface area by the multipoint method.

2.1.7. TGA analysis

The thermogravimetric diagram is obtained from a TA Instruments SDT 2960 analyzer. The temperature is raised at 10 °C/min rate from room temperature to 1000 °C under air.

2.1.8. Scanning electron microscopy

Powder morphology and average particles size were checked by field-emission scanning electron microscopy (JEOL JSM 6301F).

2.1.9. Nuclear magnetic resonance

Experiments are performed on a Bruker Avance 400 spectrometer (161.904 MHz for ^{31}P and 104.215 MHz for ^{27}Al). Quantitative ^{31}P 1D spectra are recorded using a π/2 pulse and a 60 sec delay between two pulses. The spinning speed is set to 8 or 12 KHz

Table 1
Characterization of the samples tested for the transesterification reaction.

Sample	Synthesis route	Temperature and nitridation step	Specific surface ($m^2\ g^{-1}$)	% O (wt.%)	% N (wt.%)
$AlPO_4$	Hydrogel	–	342	50.9	–
$AlPO_{3.16}N_{0.56}$	Hydrogel	800 °C—10 h	244	40.2	6.7
$AlPO_{2.93}N_{0.71}$	Hydrogel	800 °C—15 h	232	39.1	8.7
$AlPO_{2.20}N_{1.20}$	Citrate	800 °C—50 h	165	37.5	15.3

depending on the sample (12 KHz for the 15.3 wt% N sample). ^{31}P chemical shifts were referenced relative to a H_3PO_4 solution. The spinning speed for ^{27}Al NMR was set to 12 KHz with a $\pi/16$ pulse and a 0.5 s delay between two pulses. An aluminum nitrate solution was used as a reference for the chemical shifts. The separation between the contributions of the sites occupied by aluminum is often complex due to the quadrupolar feature of this atom.

2.1.10. DRIFT analysis

DRIFT spectra were collected with a FT spectrometer (Nicolet™ 380) using a deuterated triglycine sulphate (DTGS) detector working at 4 cm^{-1} resolution. The sample is placed inside a controlled environment chamber (Spectra-Tech 0030-103). Undiluted samples are heated from room temperature to 500 °C at 10 °C min^{-1} under nitrogen flow. Data are presented in absorbance mode rather than on Kubelka–Munk units because of the undiluted feature of the samples.

2.1.11. Transesterification reaction

The transesterification reaction between triglycerides and alcohols can be catalyzed by both acids and bases to prepare methyl esters of vegetable oils and a by-product glycerol [31,32]. Experiments were performed in a 100 mL stainless steel batch reactor. The reaction medium was stirred with a magnetic stirring bar and heated with a heating magnetic stirrer. Reactants (commercial alcohols and edible-grade rapeseed oil) and catalyst (0.5 g) were first introduced in the reactor. The molar alcohol/oil ratio was set at 27.5, as the nature of the alcohol could change for the study. The total mass of liquid was set at 50 g. The reaction medium was then stirred at 200 rpm and heated at 453 K. The time $t = 0$ was assigned when the temperature reached 453 K, which explains nonzero conversion at $t = 0$.

The initial reaction medium and the reaction effluents form a biphasic mixture at ambient temperature (however, it is monophasic at 453 K), the polar phase containing mainly glycerol and unreacted alcohol, and the apolar phase containing mainly FAME (or other esters when alcohols other than methanol are used) and glycerides. Sample of 2 mL were collected manually from the reaction medium, at different reaction times, for analysis. The samples were washed with brine in order to remove glycerine and the alcohol. Eight drops of the apolar phase (containing glycerides and FAME) were then diluted in 3 mL of analytical-grade THF, and the sample was analyzed by gel permeation chromatography on a Waters HPLC apparatus equipped with three Waters Styragel columns (THF) with a molar mass range of 0–1000 g mol^{-1}. These columns were placed in a thermostated oven at 313 K. Detection was made using a Waters 2414 refractive index detector. The results gave the relative composition of the apolar phase in triglycerides, diglycerides, monoglycerides, and FAME. At the end of the reaction, the reaction medium was collected and filtered on a 0.1 μm Teflon filter, and extra alcohol was evaporated. The apolar phase (containing ester and nonconverted glycerides) and the polar phase (containing glycerine and ethers) were separated and analyzed by ICP-OES, to analyze eventual catalyst leaching products. The apparatus used was a Thermo Jarrell Ash Iris Advantage inductively coupled plasma optical emission spectrometer. The apolar-phase samples were diluted in xylene and directly injected, whereas the polar-phase samples were diluted in ethanol and injected via a cold (−10 °C) nebulization chamber.

Zinc aluminate ($ZnAl_2O_4$) was chosen as a reference catalyst, as the use of this mixed oxide has been described in a heterogeneous industrial transesterification process [33].

3. Results and discussion

3.1. Preparation of nitridoaluminophosphates

$AlPO_4$ was prepared either via the hydrogel or the amorphous citrate routes. The first method usually contributed to the synthesis of $AlPO_4$, $GaPO_4$ or $AlGaPO_4$ [22,34,26]. Both synthetic approaches are efficient to prepare reactive, X-rays amorphous and high specific surface area powders. After thermal reaction under ammonia, the corresponding surface area of the oxynitride is smaller, but in a minor extent, compared to that of the precursor. Conanec showed that the evolution of the specific surface does not depend on the nitrogen enrichment, nor the reaction step under NH_3 but is rather driven by the heating kinetics of the nitridation furnace [35]. Indeed, when considering a fast heating rate, the presence of adsorbed water at the surface of the phosphate precursor will not be eliminated at low temperature and at high temperature it will follow a sintering of the powder along with a decrease in the specific surface area. Our samples were all subjected to a heating rate of 10 °C/min. The nitrogen content is essentially dependent on the nitridation step varying from 10 to 50 h. The temperature of the reaction was raised to 800 °C. Above this maximum, a release of phosphorus is observed and lead to defective compositions with ratios Al/P > 1. EDX analyses confirmed a lower phosphorus content for sample nitrided over 800 °C. Indeed, during the calcination under air at 1100 °C of oxynitride samples prepared between 800 and 1000 °C from $AlPO_4$, mixtures of $AlPO_4 + Al_2O_3$ were identified by X-rays analysis, proving the release of phosphorus throughout the nitridation treatment. The main features of these white samples prepared and tested for the transesterification reaction are gathered in Table 1.

We have selected one aluminophosphate (hydrogel route) and three nitridophosphate compositions with increasing nitrogen contents. The sample prepared with the highest nitrogen content results from a “citrate route” precursor. The purpose of this work was to study the impact of nitrogen contents and specific surface areas on the structure and the surface of the catalysts, as well as on the transesterification catalytic activity.

3.2. NMR characterizations

Due to the amorphous feature of the samples, NMR ^{31}P and ^{27}Al analyses were undertaken to characterize any modification of the aluminum and phosphorus environments with nitridation in samples listed in Table 1.

NMR ^{27}Al spectrum of $AlPO_4$ displays a major peak at 40 ppm and a second one less intensive at −10 ppm, as well as a shoulder at 10 ppm (Fig. 2). According to different authors, the main peak is attributed to aluminum in tetrahedral environment [36–40]. Taking into account the amorphous and hygroscopic behaviors of the powders, peaks at −10 and 10 ppm are linked to aluminum in

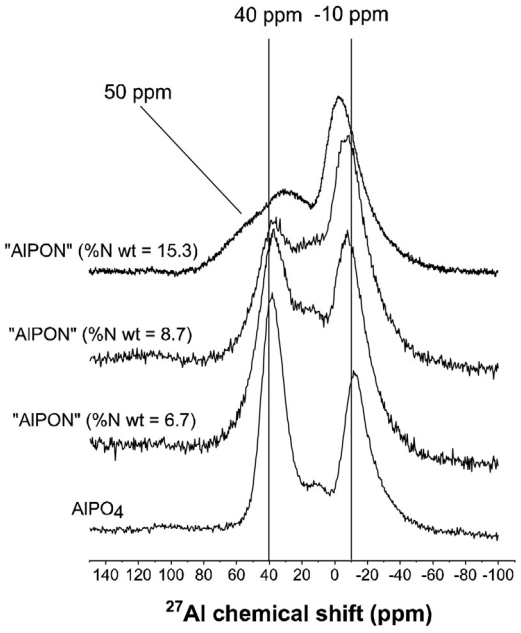

Fig. 2. NMR ^{27}Al spectra of $AlPO_4$ and corresponding oxynitrides.

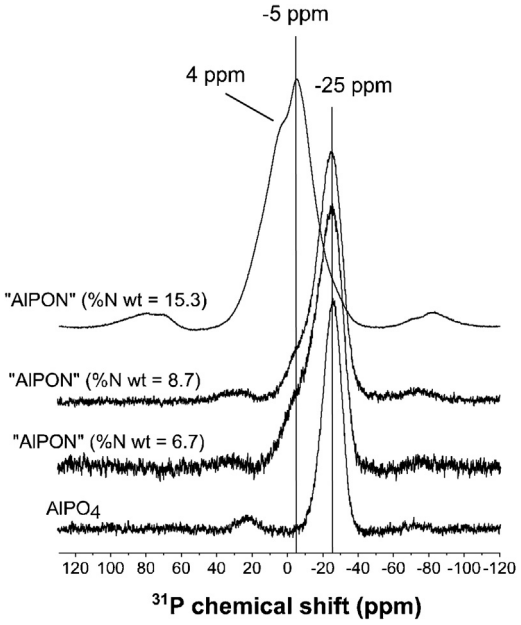

Fig. 3. NMR ^{31}P spectra of $AlPO_4$ and corresponding oxynitrides.

octahedral site and 5-fold coordinated sites respectively. Indeed, structural disorder [36,40] and/or the presence of OH groups [37,38] may involve the formation of supplementary peaks. Fig. 3 represents NMR ^{31}P spectrum of $AlPO_4$ where a single peak centered at −25 ppm corresponds to tetrahedral phosphorus $P(OAl)_4$. Peaks at 20 ppm and, in a less extent, at −70 ppm are related to the rotation bands of the rotor.

Regarding the nitrided samples, we observe on Fig. 2, with increasing nitrogen content, a progressive decrease in the intensity of the peak at 40 ppm, while no change characterizes the component at −10 ppm. The composition of the tetrahedral environment evolves continuously while the octahedral sites remain unchanged (−10 ppm). Nitrogen affects significantly only the tetrahedral environment of aluminum. For sample $AlPO_{2.20}N_{1.20}$, the tetrahedral component (40 ppm) splits clearly into two contributions one close to 30 ppm and the other at 52 ppm. This second peak was also observed by Conanec et al. for nitrided aluminophosphates containing more than 15 wt.% nitrogen [22] and assigned to a nitrided aluminum tetrahedral environment. An attempt to deconvoluate the signal of this sample gives the following quantitative distribution: 10–15% (52 ppm), 25–30% (30 ppm) and 60% (−10 ppm). But it is not obvious to do a simple determination with such a quadrupolar ^{27}Al nuclei and the presence of asymmetric peaks. This result needs therefore to be taken with precaution.

Fig. 3 indicates at low nitrogen contents the presence of a peak centered at −25 ppm (tetrahedral phosphorus) and a shoulder at −3 ppm corresponding to nitrided entities resulting from the O/N substitution. For the most nitrided sample, we observe two major peaks at 4 and −5 ppm. The component at −25 ppm attributed to PO_4 tetrahedra has nearly disappeared with significant nitrogen insertion. The component at −5 ppm may indicate the formation of PO_3N entities and the last one at 4 ppm may be related to PO_2N_2 without taking account of possible ^{27}Al-^{31}P correlations. This attribution is in agreement with the signal measured in $Na_3AlP_3O_9N$ by Stein [21]. Usually, nitrogen subsitutes for oxygen within PO_4 tetrahedra to form successively PO_3N and PO_2N_2 entities. These results confirm the work of Bunker et al. on “NaPON” glasses where the components at −20, −10 and 0 ppm were assigned respectively to PO_4, PO_3N and PO_2N_2 tetrahedra [41].

Aluminum and phosphorus atoms are principally in tetrahedral sites in $AlPO_4$ and “AlPON”. The progressive nitrogen insertion in $AlPO_4$ is followed by a displacement of the resonance signals of ^{27}Al and ^{31}P towards higher chemical shifts.

3.3. Infrared characterizations

The adsorption of probe molecules followed by infrared spectroscopy is largely used to determine the nature, the number and the force of acid and basic sites at the surface of a catalyst [42]. The evidence of the acidity is quite easy using a basic probe molecule while the determination of the basicity from acid probes is more difficult. Indeed all acid molecules may contain nucleophilic (basic) atoms interacting also with acid sites at the surface.

The IR spectrum of $AlPO_4$ in the —OH region (3000–4000 cm^{-1}) has two characteristic bands at 3796 cm^{-1} and 3679 cm^{-1} (Fig. 4). The first one is attributed to the vibrational mode of —OH groups linked to P and the second one is due to vibration modes of —OH linked to tetrahedral Al [22,43,44].

Acetonitrile (CH_3CN) is an amphoteric molecule suitable for our study to detect both acid or basic sites in the 2350–2250 cm^{-1} and 2250–2050 cm^{-1} infrared windows respectively [45]. The adsorption of acetonitrile revealed the presence of three kinds of acidic sites (2333 cm^{-1}, 2304 m^{-1} and 2274 cm^{-1}) (Fig. 5). However, it is not possible to distinguish with this probe Brønsted from Lewis acid sites. Carbon monoxyde (CO) is a basic probe and allow to differentiate between such acidic sites. The adsorption of CO at −196 °C evidences different sites of $AlPO_4$. Fig. 6 shows the bands which result from the interaction of CO with Lewis acidic sites (2215 cm^{-1}) and at least two types of Brønsted sites at 2169 cm^{-1} and 2140 cm^{-1}, which were not distinguished by ^{31}P NMR.

The introduction of nitrogen has a clear impact on the IR spectrum with the appearance of a large band centered around 3370 cm^{-1} with several shoulders between 3400 and 3600 cm^{-1}. Fig. 7 gives an illustration for the sample containing 8.7 N wt.%. This large band is attributed to the vibrational stretching modes of NHx species [46]. According to the observations of Climent et al., one of the shoulders located at 3480 cm^{-1} corresponds to NH_2 groups [47]. As for the precursor case, two fine bands at 3796 and 3676 cm^{-1} indicate the presence of hydroxyl groups linked respectively to aluminum and phosphorus atoms in tetrahedral sites. With increasing nitrogen content, we note a decrease in the relative intensity

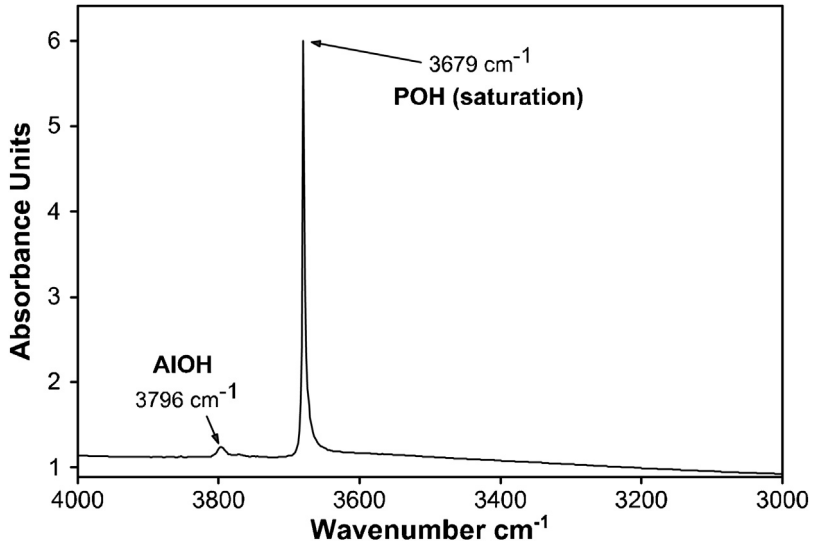

Fig. 4. IR spectrum of $AlPO_4$.

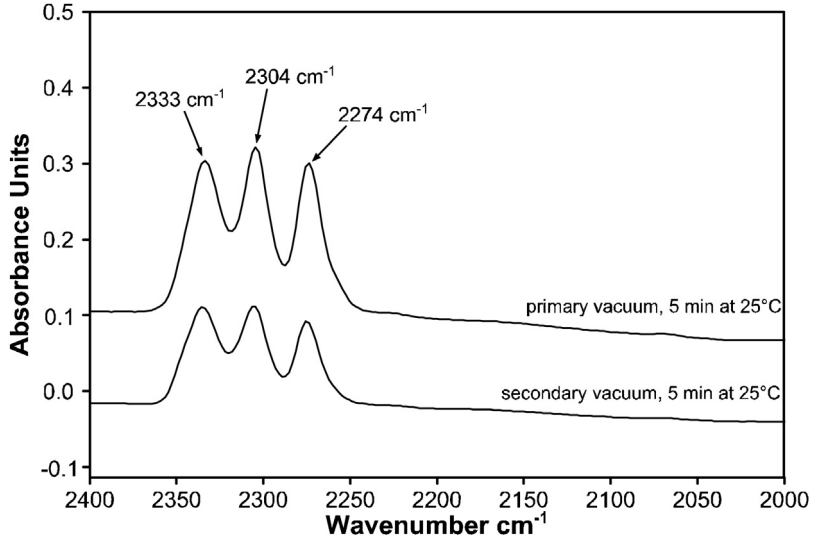

Fig. 5. Adsorption of acetonitrile on $AlPO_4$ sample.

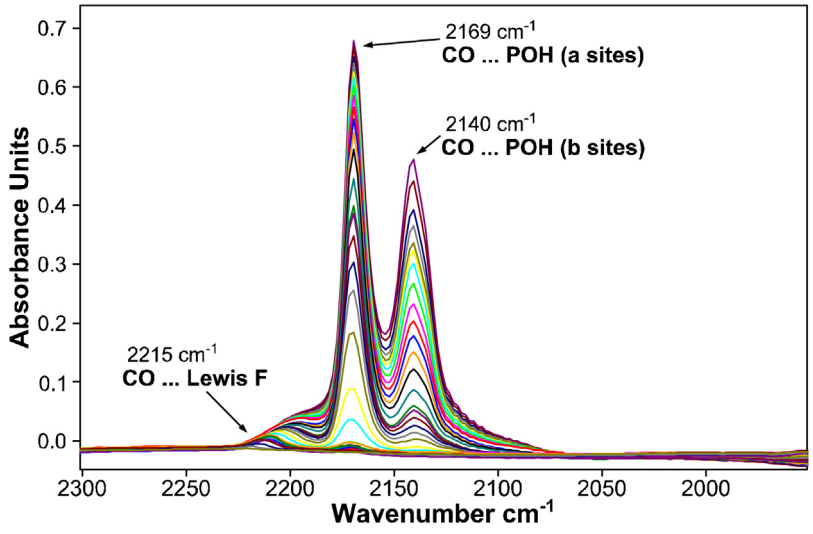

Fig. 6. Adsorption of CO on $AlPO_4$ surface.

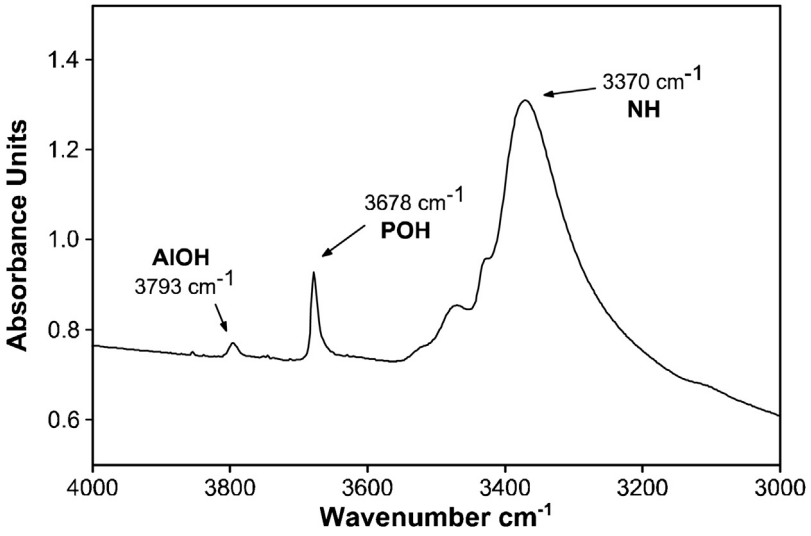

Fig. 7. IR spectrum of AlPON (8.7 N wt.%).

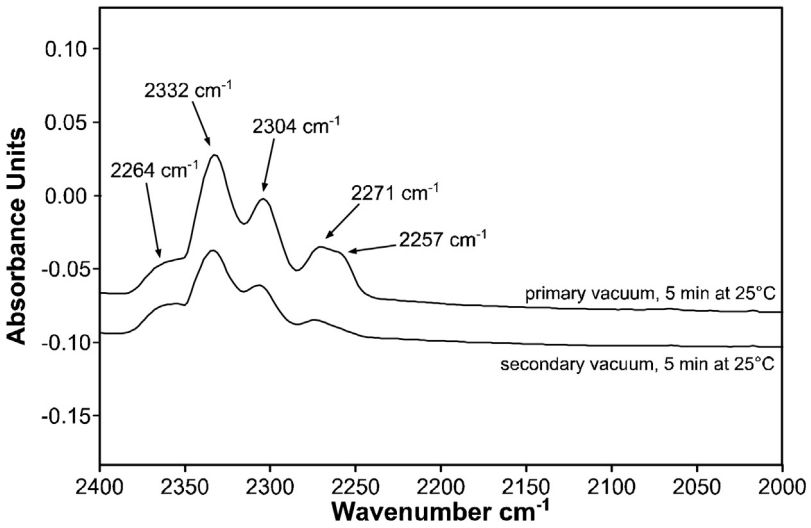

Fig. 8. Adsorption of acetonitrile on AlPON—8.7 N wt.% sample.

of ν_{PO-H} band (around 3680 cm^{-1}) compared with ν_{AlO-H} band. Ammonia interacts preferentially with P—OH sites at the surface of the aluminophosphates to form P-NHx species.

With acetonitrile adsorption we observe for the nitrided sample (6.7 N wt.%) the same bands (2335, 2305 and 2272 cm^{-1}) related to acid sites as displayed by the oxide precursor (Fig. 5). By comparison with $AlPO_4$, the intensity of the bands at 2272 and 2305 cm^{-1} are less intensive, proving the influence of the nitridation on some of these acid sites. With increasing nitrogen content, a supplementary band (acid site) is detected at 2364 cm^{-1} (2257 cm^{-1} is a physisorption band) (Fig. 8). The adsorption spectrum of acetonitrile on the sample with 15.3 N wt.% is quite different from the others, with the presence of only two acidic sites at 2329 cm^{-1} and 2301 cm^{-1}.

It has to be noticed that no basic sites were evidenced neither by acetonitrile adsorption or CO_2 adsorption (not shown). This probe molecules could not be efficient to reveal the basic sites of AlPON, revealed otherwise by the presence of —NHx groups visible in the IR spectrum.

The adsorption of CO on nitrided samples confirms the presence of two types of acidic sites. A Lewis site at 2203 cm^{-1} and three Brønsted sites at 2167, 2152 and 2140 cm^{-1}. The nitridation also modifies the profile of the Brønsted acidity region around 2150 cm^{-1} in intensity (maybe linked to the modification of extinction coefficient or to a lower number of acid sites, as it can be thought regarding the decrease of the P—OH band intensity) and with the appearance of a band at 2152 cm^{-1} (Fig. 9).

With higher nitrogen content (8.7 N wt.%) the spectra display two Lewis sites 2218 and 2196 cm^{-1} and three Brønsted sites (2168, 2154, 2140 cm^{-1}). At higher nitrogen content (15,3 N wt.%) the CO adsorption spectrum indicates a very weak proportion of Lewis acidic sites (2193 cm^{-1}) compared with Brønsted sites at 2169, 2149 and 2138 cm^{-1} (Fig. 10).

If the presence of acid centers in the aluminophosphates was evidenced for both oxide and oxynitride catalysts, basic sites are more difficult to characterize. Infrared spectroscopy with acetonitrile adsorption never reveals, under our experimental conditions, basic sites and moreover the basicity was not even shown through our CO_2 TPD experiments. Despite of this impossibility to clearly detect basic sites, we have tested these (nitrido) aluminophosphates in heterogeneous catalysis for the transesterification reaction in order to study the influence of the nitrogen content on the catalytic activities.

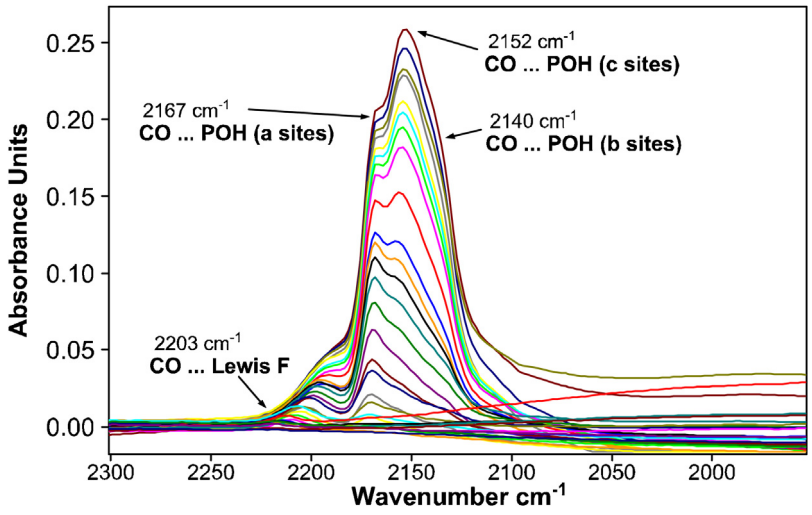

Fig. 9. Adsorption of CO on AlPON—6.7 N wt.% sample.

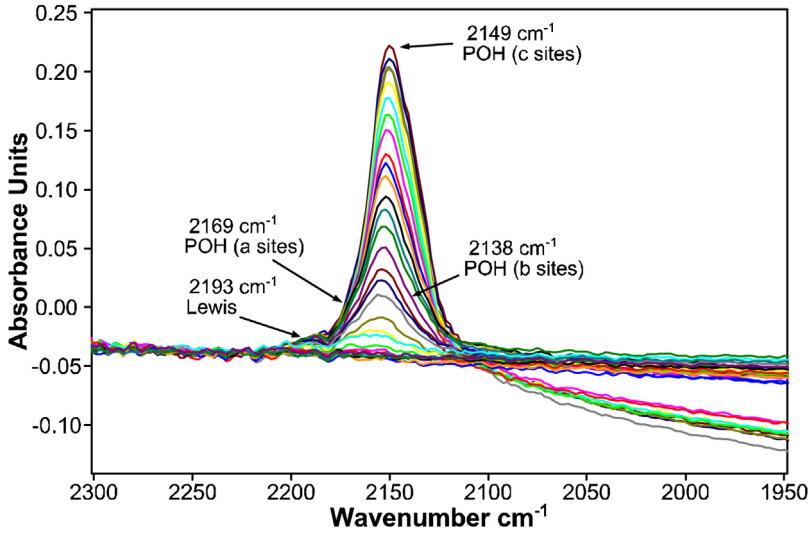

Fig. 10. Adsorption of CO on AlPON—15,3 N wt.% sample.

3.4. Catalytic activity for the transesterification reaction

A large part of the production of biodiesel is performed using soluble basic homogeneous catalysts, i.e. sodium hydroxide or sodium methoxide. In this case, the alcohol is deprotonated by the base and transformed into an alcoholate. However, several purification steps are necessary to reach a high level of purity for the targeted esters (biodiesel) and glycerine in agreement with the required standards. Indeed, glycerine is polluted with alkali salts or alcoholates so that the purification process has a major cost of the same order of that necessary to prepare esters.

Unlike homogeneous catalysts, heterogeneous catalysts present the appreciable advantage to produce esters and glycerine without any trace of catalyst which make them easier to purify. Basic heteregoneous catalyst based on zinc aluminate is the core of the IFPEN/Axens Esterfip-H® process, which is the only industrial heteregenous catalyst for the transesterification of vegetable oils. This basic heterogeneous catalyst allows high activities as well as high selectivities for a high glycerine purity. Acid catalysts tend to be more active, but the formation of ethers is possible due to the presence of Brönsted acid sites at their surface, thus degrading the overall selectivity of the reaction.

In order to take advantage of the two types of heterogeneous catalysts—acid and basic—in the transesterification reaction, nitridophosphates $AlPO_xN_y$ are catalysts of choice for which the acido–basicity can be modified by tuning the nitrogen content in these solid solutions.

Looking at the different steps of the reaction (Fig. 11), the formation of glycerine occurs only after three consecutive transesterification reactions of triglycerides into diglycerides and monoglyceride and the formation of the third fatty acid methyl ester (FAME) molecule. Our study was conducted as much as possible in agreement with the European specification EN 14214 (2003) relative to the impurities content: FAME should contain at least 96.5 wt.% esters, less than 0.8 wt.% monoglycerides, 0.2 wt.% diglycerides and 0.2 wt.% triglycerides, few free fatty acids (<0.5 mg KOH/g) that can be corrosive, less than 0.25 wt.% glycerine and only metals as traces.

The catalytic activity was measured for all samples according to the procedure described in the experimental section. Fig. 12 displays diverse catalytic behaviors for the triglycerides conversion depending on the tested catalyst among $ZnAl_2O_4$ (spinel-type), the oxide $AlPO_4$ and three oxynitrides $AlPO_xN_y$ with different anionic contents. $ZnAl_2O_4$ is a basic reference catalyst known for its high

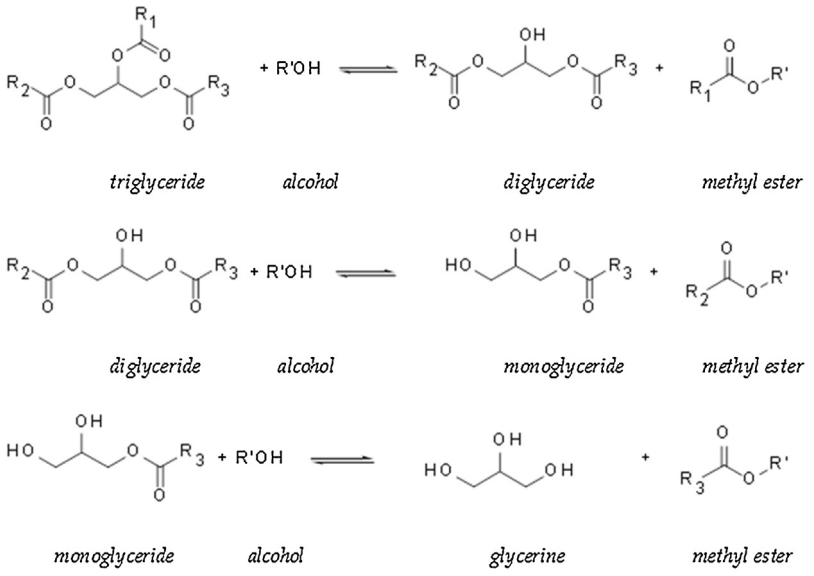

Fig. 11. Transesterification reaction scheme.

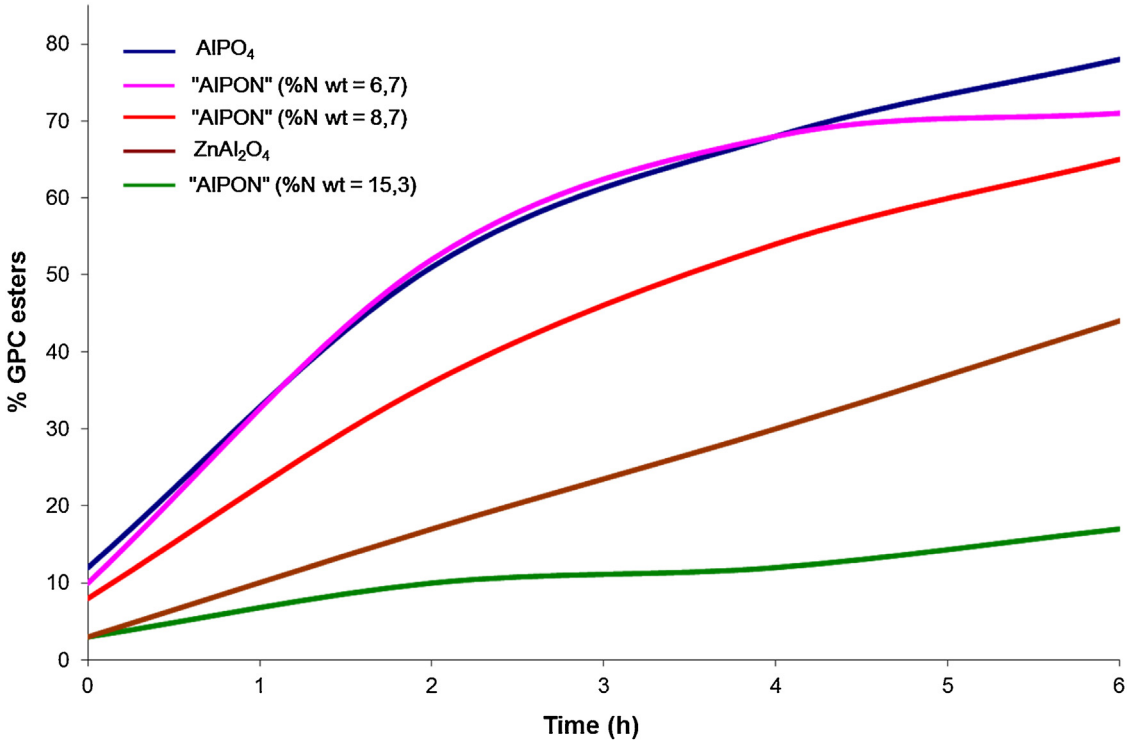

Fig. 12. Triglycerides conversion rates with different catalysts vs. time.

stability during the transesterification. At first sight, the most active catalyst is $AlPO_4$ with a conversion rate of 77% after only 6 h of reaction. With increasing nitrogen content, we observe a decrease in the conversion rate of the triglycerides into methyl esters. The most nitrided sample with $N = 15.6\%$ presents only a yield of 16% after 6 h reaction.

Table 2 reports on the progressive weight evolution of the entities remaining in the reactor after few hours when the oxide $AlPO_4$ is used as a catalyst. We observe clearly the consumption of the triglycerides (canola oil) towards the synthesis of methyl esters (FAME). An initial conversion (at $t = 0$) is observed because the reac-

Table 2
Triglycerides conversion in presence of $AlPO_4$.

		Sampling (h)			
		0[b]	2	4	6
wt.% in the organic phase[a]	Triglycerides	73	34	20	12
	Diglycerides	12	11	7	5
	Monoglycerides	2	4	5	6
	FAME	13	51	68	77

[a] Determined by GPC.
[b] $t = 0$ when the experimental device reaches 180 °C.

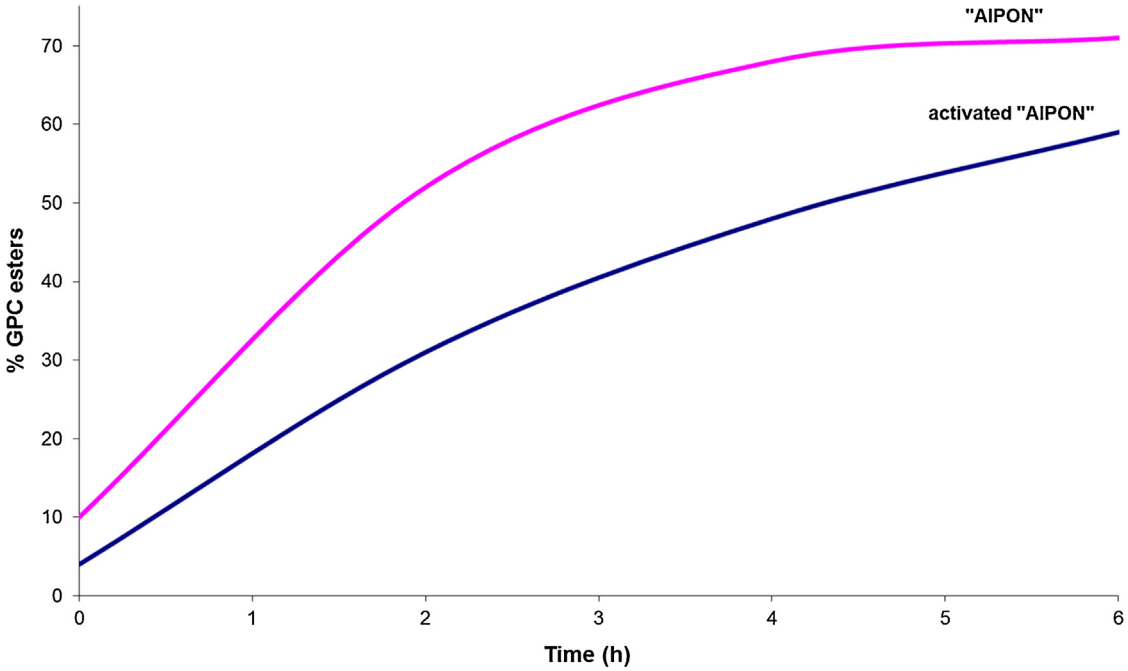

Fig. 13. "AlPON" (N wt.% = 6.7) activation under vacuum.

tion starts before the experiment reaches the reaction temperature of 180 °C.

Compared to the performance of the reference $ZnAl_2O_4$ (Table 3), the $AlPO_4$ catalyst exhibits a much higher conversion yield of triglycerides into FAME.

However, after reaction, the resulting glycerine presents a high ether (methoxyglycerol and dimethoxyglycerol) content close to 16 wt.%. It is necessary to limit drastically the formation of such phases to keep a high level of purity. In order to combine both an important production of FAME and high purity glycerine, nitrided-$AlPO_4$ catalysts were tested under the same experimental conditions. Despite of a lower conversion rate observed on Fig. 12 ($AlPO_xN_y$ 6.7 and 8.7 wt.% N), the ether content measured in the glycerine phase is considerably lower (<0,1%), suggesting a high purity. Thus, the insertion of nitrogen was efficient to modify the acido–basicity of the surface of the catalyst and to orientate the reaction towards pure final products.

The use of $AlPO_xN_y$ oxynitrides allows to attain significant catalytic results, 70% and 65% conversion rates for the samples containing 6.7 and 8.7 wt.% nitrogen respectively. For this transesterification reaction both acid and basic sites are active to catalyse the reaction, but each of them manifests a different selectivity. Basic

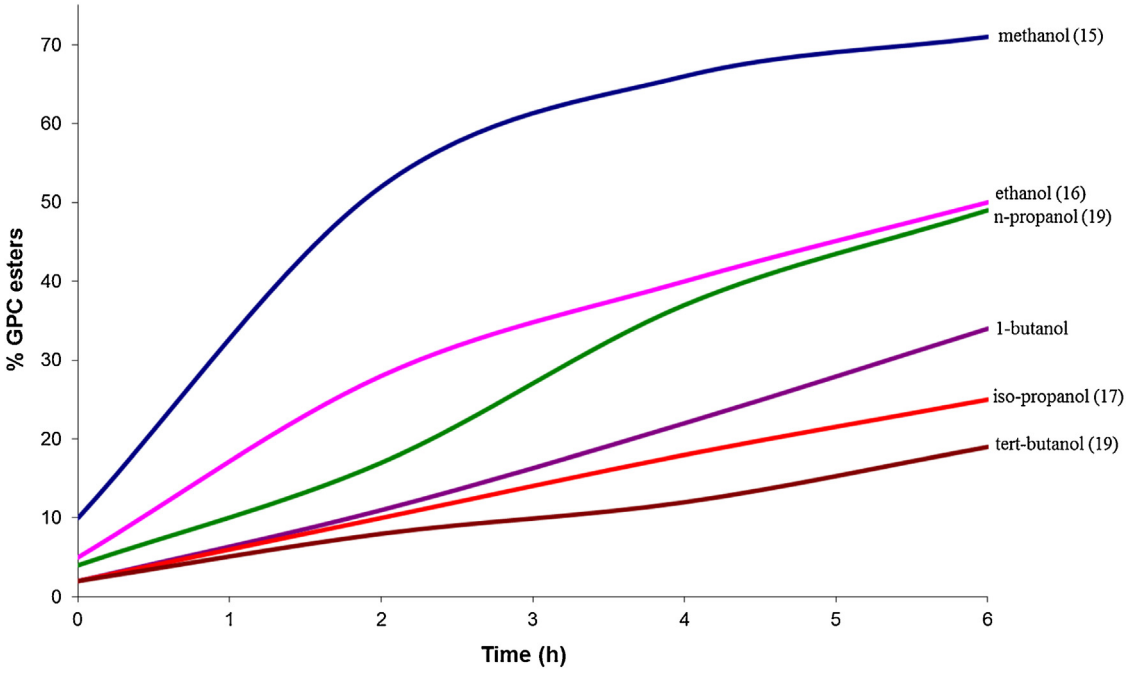

Fig. 14. Activity of the catalyst "AlPON" (N wt.% = 6.7) vs. a panel of alcohols.

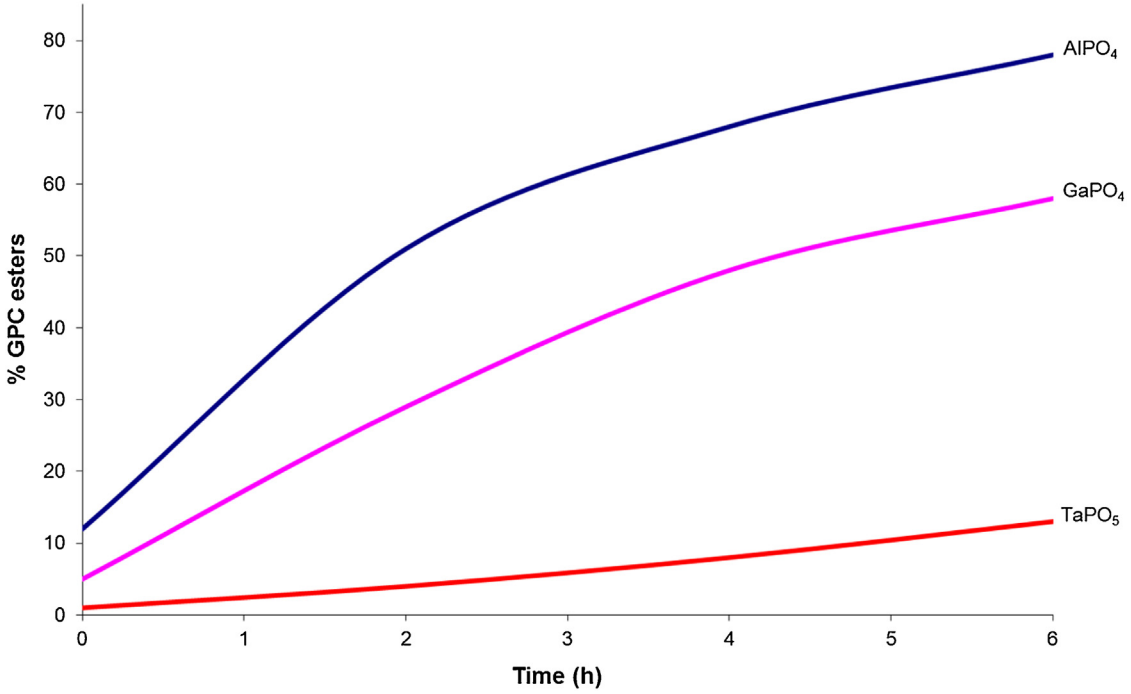

Fig. 15. Catalytic activities vs. different cations.

Table 3
Triglycerides conversion in presence of $ZnAl_2O_4$.

		Sampling (h)		
		0[b]	4	6
wt.% in the organic phase[a]	Triglycerides	92	44	29
	Diglycerides	5	20	18
	Monoglycerides	0	7	9
	FAME	3	29	44

[a] Determined by GPC.
[b] $t = 0$ when the experimental device reaches 180 °C.

Table 4
Velocity constant of the reaction (triglycerides conversion) per unit of surface.

Catalyst	$k\ (s^{-1}\ m^{-2}) \times 10^4$
AlPON 6.7% nitrogen	24
AlPON 8.7% nitrogen	19
$AlPO_4$	17
$ZnAl_2O_4$	11
AlPON 15.3% nitrogen	7

catalysts are the most selective whereas acid ones lead often to the formation of glycerol ethers affecting the formation of glycerine. Moreover, Lewis acid sites are more active for transesterification while Brönsted one are less selective. The ideal case is to favor the creation of Lewis acid sites and basic sites. Unfortunately, the comprehension of the formation of Lewis and Brönsted acid sites is really difficult; nitrogen seems however to impact some acid sites and contributes to the formation of basic sites.

The increase of the nitrogen content may be correlated to the reaction time and the ensuing decrease of the specific surface area, which one influences the catalytic activity through the number of active sites. In Table 4 are reported the kinetics constants related to the transformation of triglycerides by considering the hypothesis: the methanol concentration is kept constant and iso-mass compared to triglycerides. These constants are calculated per unit of surface to avoid any effect of BET surface variation.

Nitridophosphates $AlPO_xN_y$ with 6.7 and 8.7 wt.% nitrogen are characterized by the highest velocity constants in comparison with their oxide precursor although their catalytic activities are lower (see Fig. 12). The catalyst with 15.3 wt.% nitrogen is less efficient than $ZnAl_2O_4$. This observation indicates finally that in the iso-mass conditions the triglycerides conversion is more important when using $AlPO_xN_y$ catalysts, although a too much important nitrogen substitution may involve a decrease in the catalytic activity. This assumption does not take account of the powder morphology that controls also the catalysis reaction.

These phosphate catalysts are stable in the reactor. No leaching was reported (dissolution of the catalyst in the formed phases). Indeed, in the ester phase, the aluminum content is lower than 1 ppm and phosphorus lower than 5 ppm. In the glycerine, aluminum and phosphorus are measured between 10 and 50 ppm. This rate is even lower than 10 ppm for phosphorus originating from $AlPO_4$ catalyst. Thus, both esters and glycerine we aim to prepare are of a high purity, except when using $AlPO_4$ where noxious ethers are formed.

As the acido–basic sites are extremely sensitive to air and water, a catalytic test was performed first by activating $AlPO_xN_y$ catalysts (with 6.7 wt.% N) under vacuum for 2 h, and then they were loaded in the reactor under inert atmosphere (Fig. 13).

The activated catalyst appears less active than that stored in air without any precaution. This difference may be explained by the disappearance of some acido–basic sites (hydroxyles, carbonates...) due to the pretreatment. These sites of medium or weak strength may be active in transesterification. This hypothesis was not proven by infrared study because the activation is needed to substract the water signal.

3.4.1. *Influence of the reacting alcohol*

The impact of the choice of the alcohol to react with the vegetable oils in presence of the catalyst AlPON (6.7 wt.% N) is shown on Fig. 14. Quantities of alcohol and vegetable oils have been adapted in order to keep a molar ratio alcohol/oil = 27.5 and a total mass of 50 g. The pK_a of each alcohol/alcoholate couple is given in brackets.

Table 5
Triglycerides conversion kinetics constants per unity of surface.

Catalyst	Specific surface ($m^2\ g^{-1}$)	$k\ (s^{-1}\ m^{-2}) \times 10^4$
$AlPO_4$	340	17
$GaPO_4$	130	31
$TaPO_5$	280	4
$ZnAl_2O_4$	–	11

These results point out a significant difference in activities between methanol and other alcohols. During the reaction, the catalyst (acid and/or basic) should be able to deprotonate the alcohol to form FAME. Depending on the chosen alcohol and its pK_a, the catalysts—acid or basic—will not have the same ability to deprotonate.

Thus, as AlPON is an acid–base catalyst, the transesterification reaction may be driven by a basic or acid–base mechanism. The difference between ethanol and *n*-propanol is quite small regarding the activities, an acid mechanism may characterize them. Indeed, despite of an important pK_a difference, the esters yield are similar. It seems that the reaction does not require the deprotonation of the alcohol on a basic site. The steric hindrance within the alcohols affect also the catalytic activity as branched alcohols lead only to poor conversion rates (less than 20% esters within 6 h with *tert*-butanol).

3.4.2. *Influence of the cation*

Considering the substantial results measured for the catalytic activities of aluminophosphates ($AlPO_4$ et "AlPON") for the transesterification reaction, more phosphates based on different cations have been prepared and evaluated in the same conditions, for example $GaPO_4$ and $TaPO_5$ whose results are reported on Fig. 15. The main characteristics for this test are given in Table 5.

In similar experimental conditions, $AlPO_4$ presents the best activity (conversion of 77%), $GaPO_4$ produces a conversion of 58% while $TaPO_5$ only13 %.

Converted per unit of surface, $GaPO_4$ offers the highest conversion kinetics constant (Table 5). Group III based phosphates (with Al and Ga) are active for the transesterification reaction. Tantalum-based phosphate does not have any interest for this reaction. Titanium was also tested with TiPON samples, but unfortunately give rise to an important leaching where the catalysts is dissolved at the end of the reaction.

4. Conclusion

Nitridoaluminophosphates have been prepared with different nitrogen contents (from 6 to 15 wt.%) and their spectroscopic characterizations were performed using infrared and NMR. Infrared analyses indicate the presence of Lewis and Brønsted sites at the surface of all catalysts. Although the basicity of AlPON was evidenced by CO_2 TPD (Conanec et al.), no basic sites was properly detected on the nitrided phases under our experimental conditions. ^{31}P and ^{27}Al NMR studies show that phosphorus and aluminum atoms are mainly in tetrahedral sites of the "AlPON" structure. The progressive nitridation of $AlPO_4$ results in the shift of the resonance peaks towards higher chemical shifts, a typical feature encountered with nitrogen insertion.

$AlPO_4$ used as an acid catalyst provided the best catalytic activity compared to nitrided phosphates. However the triglycerides conversion velocity constants (per unit of surface) prove that some of the AlPON catalysts (containing 6.7 and 8.7 wt.% N) are more efficient for the transesterification reaction. The insertion of nitrogen within an acid catalyst has an impact on acid sites and more than likely on the formation of basic sites. Moreover acid catalysts like $AlPO_4$ lead to the formation of ethers that impair the quality of glycerine, but AlPONs bring a solution to overcome this pollution without affecting conversion rates. The choice of the alcohol and the cation plays a major role on the values of the conversion rates. AlPONs accommodate very well with methanol. $AlPO_xN_y$ nitridophosphates, with tunable acido–basicity, produced significant better catalytic results in comparison with a $ZnAl_2O_4$ catalyst reference.

Acknowledgments

This work was supported by the Région Bretagne for an ARED doctoral grant (ARED 08005896). The authors thank Anne-Agathe Quoineaud and Emmanuel Soyer from IFPEN for fruitful discussions.

References

[1] J.B. Moffat, Topics Phosphorus Chem. 10 (1980) 285.
[2] J.B. Moffat, Catal. Rev. 18 (2) (1978) 199.
[3] K.K., Kearby, Proc. 2nd. Int. Catal. Cong., Editors Technip, Paris, 1961, 2567.
[4] W.J., Mattex, Esso Research and Engineering Company, Brevet Fr-A-2 0077 099, 1971.
[5] K.K., Kearby, Esso Research and Engineering Company, US Patent 3 342 750, 1967.
[6] P.M. Deya, A. Costa, J.V. Sinisterra, J.M. Marinas, Can. J. Chem. 60 (1982) 35.
[7] J.M. Campelo, A. Garcia, J.M. Guttierez, D. Luna, J.M. Marinas, Can. J. Chem. 61 (1983) 2567.
[8] A. Blanco, J.M. Campelo, A. Garcia, D. Luna, J.M. Marinas, A.A. Romero, J. Catal. 137 (1992) 51.
[9] A. Schmidtmeyer, J.B. Moffat, J. Catal. 96 (1985) 242.
[10] M.J. Climent, A. Corma, R. Guil-Lopez, S. Iborra, J. Primo, Catal. Lett. 59 (1999) 33–38.
[11] M.J. Climent, A. Corma, R. Guil-Lopez, S. Iborra, J. Primo, Catal. Lett. 74 (2001) 161–167.
[12] M. Hasni, J. Rouchaud, P. Grange, M. Devillers, S. Delsarte, Mater. Sci. Forum 554 (2007) 37–42.
[13] M. Montes, M. Martin, A. Diaz, J.J. Benitez, J.A. Odriozola, Mater. Sci. Forum 325–326 (2000) 83–90.
[14] M. Hasni, G. Prado, J. Rouchaud, P. Grange, M. Devillers, S. Delsarte, J. Mol. Catal. A Chem. 247 (2006) 116–123.
[15] S. Delsarte, F. Maugé, P. Grange, J. Catal. 202 (2001) 1–13.
[16] S. Delsarte, P. Grange, Appl. Catal. A 259 (2004) 269–279.
[17] S. Delsarte, M. Florea, F. Maugé, P. Grange, Catal. Today 116 (2006) 216–225.
[18] L.M. Gandia, R. Malm, R. Marchand, R. Conanec, Y. Laurent, M. Montes, Appl. Catal. A 114 (1) (1994) 1–7.
[19] P. Grange, P. Bastians, R. Conanec, R. Marchand, Y. Laurent, Appl. Catal. A 114 (2) (1994) 191–196.
[20] E. Gueguen, S. Delsarte, V. Peltier, R. Conanec, R. Marchand, Y. Laurent, J. Eur. Ceram. Soc. 17 (15–16) (1997) 2007–2010.
[21] A. Stein, B. Wehrle, M. Jansen, Zeolites 13 (1993) 291.
[22] R. Conanec, Thesis n°1278, Université de Rennes 1, France, 1994;
J.J. Benitez, P. Malet, P.I. Carrizosa, J.A. Odriozola, R. Conanec, R. Marchand, Y. Laurent, J. Eur. Ceram. Soc. 17 (15–16) (1997) 1979;
A. Massinon, E. Gueguen, R. Conanec, R. Marchand, Y. Laurent, P. Grange, Stud. Surf. Sci. Catal. 101 (1996) 77;
A. Massinon, J.A. Odriozola, P. Bastians, R. Conanec, R. Marchand, Y. Laurent, P. Grange, Appl. Catal. A Gen. 137 (1) (1996) 9;
P. Grange, P. Bastians, R. Conanec, R. Marchand, Y. Laurent, L. Gandia, M. Montes, J. Fernandez, J.A. Odriozola, Stud. Surf. Sci. Catal. 91 (1995) 381;
L.M. Gandia, R. Malm, R. Marchand, R. Conanec, Y. Laurent, M. Montes, Appl. Catal. A Gen. 114 (1) (1994) L1;
R. Conanec, R. Marchand, Y. Laurent, P. Bastians, P. Grange, Mater. Sci. Forum 152–153 (1994) 305;
R. Marchand, R. Conanec, E. Gueguen, Y. Laurent, Phosphorus Sulfur Silicon Relat. Ele. 76 (1–4) (1993) 537.
[23] A. Corma, R.M. Martin-Aranda, Appl. Catal. A Gen. 105 (1993) 271.
[24] J. Lopez-Gonzalez, A. Lopez-Peinado, E.M. Martin-Aranda, M.L. Rojas-Cervantes, Carbon 31 (8) (1993) 1231.
[25] K.K., Kearby, Proc. 2nd Int. Congr. Catal. Paris, Technip 1961, 2567–2578.
[26] V. Peltier, Thesis n°1897, Université de Rennes 1, France, 1997;
S. Delsarte, V. Peltier, Y. Laurent, P. Grange, Stud. Surf. Sci. Catal. 118 (1998) 869;
V. Peltier, R. Conanec, R. Marchand, Y. Laurent, S. Delsarte, E. Gueguen, P. Grange, Mater. Sci. Eng. B Solid State Mater. Adv. Technol. B47 (2) (1997) 177.
[27] E. Ray, F. Tessier, N. Herbert, R. Lebullenger, C. Roiland, B. Bureau, J. Alloys Comp. 513 (2012) 530–538.
[28] A. Douy, P. Odier, Mater. Res. Bull. 24 (1989) 1119–1126.
[29] F. Tessier, R. Marchand, J. Solid State Chem. 171 (2003) 143–151.
[30] W. Gruner, B. Wollein, W. Lengauer, Microchim. Acta 146 (2004) 1–6.
[31] S. Gryglewicz, Bioresour. Technol. 70 (1999) 249–253.

[32] U. Schuchardt, R. Sercheli, R. Matheus Vargas, J. Braz. Chem. Soc. 9 (1998) 199–210.
[33] V. Pugnet, S. Maury, V. Coupard, A. Dandeu, A.-A. Quoineaud, J.-L. Bonneau, D. Tichit, Appl. Catal. A 374 (2010) 71–78.
[34] V. Peltier, R. Conanec, R. Marchand, High Temp. Mater. Processes (N. Y.) 1 (2) (1997) 287–293.
[35] R. Conanec, R. Marchand, Y. Laurent, High Temp. Mater. Processes 1 (1992) 157–164.
[36] T.P.P. Cheung, K.W. Willcox, M.P. McDaniel, M.M. Johnson, C. Bronniman, J. Fry, J. Catal. 102 (1986) 10.
[37] R. Glemza, Y.O. Parent, W.A. Welsh, Catal. Today 14 (1992) 175.
[38] G.P. Babu, P. Ganguli, K. Metcalfe, J.W. Rockliffe, E.G. Smith, J. Mater. Chem. 4 (2) (1994) 331.
[39] D. Muller, I. Grunze, E. Hallas, G. Ladwig, Z. Anorg. Allg. Chem. 500 (1983) 80.
[40] R. Brow, R. Kirkpatrick, G. Turner, J. Am. Ceram. Soc. 76 (4) (1993) 919.
[41] B. Bunker, D. Tallant, C. Balfe, R. Kirkpatrick, G. Turner, M. Reidmeyer, J. Am. Ceram. Soc. 70 (9) (1987) 675.
[42] J.C. Lavalley, Catal. Today 27 (1996) 377–401.
[43] B. Rebenstorf, T. Lindblad, L.T. Andersson, J. Catal. 128 (1991) 293.
[44] J.B. Moffat, Catal. Rev. Sci. Eng. 18 (1978) 199.
[45] O. Lorret, S. Morandi, F. Prinetto, G. Ghiotti, D. Tichit, R. Durant, B. Coq, Microporous Mesoporous Mater. 103 (2007) 48–56.
[46] J.J. Benítez, A. Díaz, Y. Laurent, J.A. Odriozola, Appl. Catal. A 176 (1999) 177–187.
[47] M.J. Climent, A. Corma, V. Fornés, A. Frau, R. Guil-López, S. Iborra, J. Primo, J. Catal. 163 (1996) 392–398.